

3D RECONSTRUCTION OF AN UNDERWATER ARCHAEOLOGICAL SITE: COMPARISON BETWEEN LOW COST CAMERAS

A. Capra^{a*}, M. Dubbini^b, E. Bertacchini^a, C. Castagnetti^a, F. Mancini^a

^a DIEF, Dept. Engineering “Enzo Ferrari”, University of Modena e Reggio Emilia, via Pietro Vivarelli 10/1, 41125 Modena, Italy – (alessandro.capra, eleonora.bertacchini, cristina.castagnetti, francesco.mancini)@unimore.it

^b DiSCi, Dept. History Culture Civilization - Headquarters of Geography, University of Bologna, via Guerrazzi 20, 40125 Bologna, - (marco.dubbini@unibo.it)

Commission V

KEY WORDS: Photogrammetry, Underwater, 3D reconstruction, Archaeological, Calibration and Orientation, Cultural Heritage

ABSTRACT:

The 3D reconstruction with a metric content of a submerged area, where objects and structures of archaeological interest are found, could play an important role in the research and study activities and even in the digitization of the cultural heritage. The reconstruction of 3D object, of interest for archaeologists, constitutes a starting point in the classification and description of object in digital format and for successive fruition by user after delivering through several media. The starting point is a metric evaluation of the site obtained with photogrammetric surveying and appropriate 3D restitution. The authors have been applying the underwater photogrammetric technique since several years using underwater digital cameras and, in this paper, digital low cost cameras (off-the-shelf). Results of tests made on submerged objects with three cameras are presented: © Canon Power Shot G12, © Intova Sport HD e © GoPro HERO 2. The experimentation had the goal to evaluate the precision in self-calibration procedures, essential for multimedia underwater photogrammetry, and to analyze the quality of 3D restitution. Precisions obtained in the calibration and orientation procedures was assessed by using three cameras, and an homogeneous set control points. Data were processed with © Agisoft Photoscan. Successively, 3D models were created and the comparison of the models derived from the use of different cameras was performed. Different potentialities of the used cameras are reported in the discussion section. The 3D restitution of objects and structures was integrated with sea bottom floor morphology in order to achieve a comprehensive description of the site. A possible methodology of survey and representation of submerged objects is therefore illustrated, considering an automatic and a semi-automatic approach.

1. INTRODUCTION

The seabed is often defined as "the greatest museum in the world." The underwater cultural heritage includes all traces of human existence that lie beneath the water and have a cultural or historical character. Entire cities have been swallowed up by the waves, and thousands of ships have been lost at sea. While these ships, buildings and historical objects are not visible on the surface, their remains have survived to the bottom of lakes, seas and oceans stored safely in the aquatic environment. This heritage includes three million ancient shipwrecks, their content, submerged ruins, cities and thousands of prehistoric sites. In 2001, UNESCO, given the urgent need to preserve and protect this heritage submerged, drafted the "Convention on the Protection of Underwater Cultural Heritage". So that everyone can benefit from this immense underwater cultural heritage (both the visitor that the technician), in recent years the reproduction of digital three-dimensional models with high resolution and high geometric accuracy, is the methodology that is being adopted. The underwater photogrammetric technique appears to be the most appropriate methodology for this purpose. One major reason is that related to the fact of not coming into contact with the object. This is very important for the preservation of the object within its natural environment. For a pure geometric description one could also think of techniques based on acoustic methods, but there would not be

the description of the object color (texture), which appears to be essential for many types of studies.

The underwater photogrammetry is a technique that since the year 80 is effective for the geometric description of submerged objects (Capra, 1992; Troisi et al., 2013). The main goal is the determination of the interior orientation parameters of the camera because of multimedia resources (water, glass, air, lenses, air).

This article focuses on the definition of the parameters of interior orientation of three types of cheap camera (© Canon Power Shot G12, © Intova Sport HD e © GoPro HERO 2), comparing them after their determination using photogrammetric algorithms, very often implemented by the computer vision sciences (for instance the Structure from Motion with bundle adjustment), and a commercial software (PhotoScan, ©Agisoft)

2. THE INVESTIGATION SITE

The study site was selected after the discovery of an amphora from the Roman period, type Dressel 1B (Caravalle, 1997), in the Middle Shoal Channel - Porto San Paolo - Olbia (Italy), Area C of the marine protected area, at 15m of depth. See Figure 1 as location map. Figure 2 represents the Dressel Table, reporting a classification of amphoras based on shapes. Figure 3 depicts the amphora Dressel B1 as visible on the seabed.

* Corresponding author

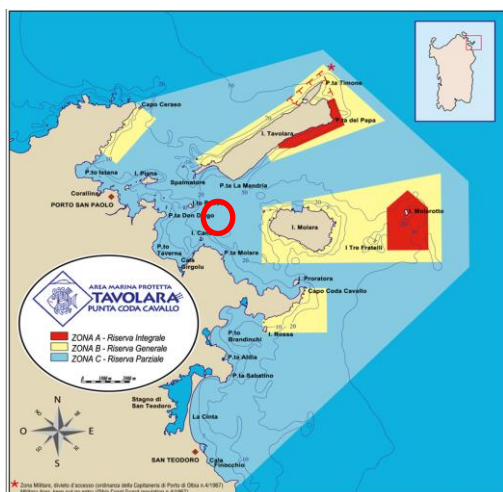


Figure 1. Site of Operation

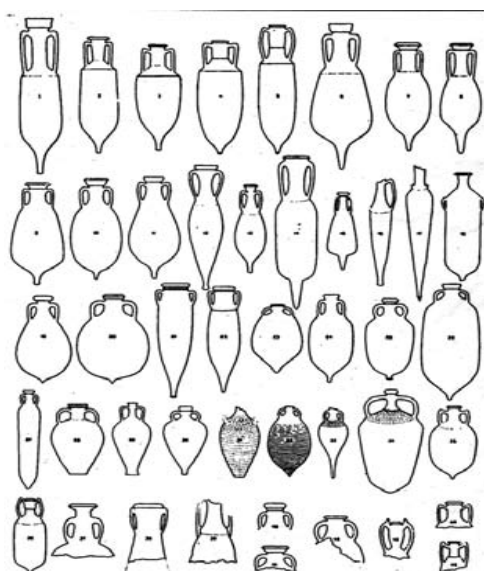


Figure 2. Dressel Table



Figure 3. Amphora Dressel B1 on the seabed

3. USED CAMERAS

As said, 3 different low cost cameras were used for this test in order to assess their reliability under the operational conditions. In Table 1, Table 2 and Table 3 the main characteristics of the used cameras.

© Canon Power Shot G12:

Image Sensor	CCD	1 / 1.7"
Resolution	10M	3648 x 2736 pixel 12211.538 dpi
Focal Length	from 6,1 to 30,5 mm (equivalent a 35 mm: 28 - 140 mm)	
Zoom	5x Optical. Digital approx circa 4x (with digital teleconverter approx 1,4x o 2,3x e Safety Zoom ¹) ² . Approximately 20x	
Opening Maximum	f/2,8-f/4,5	
Flash	Present. With the possibility of the external Flash	
Supported Operating System	Windows 7/ Vista SP1-2/ XP SP3 Macintosh - Mac OS X v10.4-10.6 (Intel processor required)	
Operating Environment	From 0 a -40°C Humidity 10 to 90 %	
Dimension	112.1 x 76.2 x 48.3 mm without underwater housing	
Weigh	About 401 g without underwater housing	

Table 1. Main characteristics of Canon camera

© Intova Sport HD

Image Sensor	C-MOS	1 / 2.3"
Resolution	12M	4000 x 3000 pixel
	8 M	3200 x 2400 pixel
Focal Length	5.0 mm	
Zoom	Digital zoom 4x (no zoom mode 1080P)	
Opening Maximum	f/3.6 – wide angle lens 140°	
Flash	Not present	
Supported Operating System	Windows 2000/ XP/ Vista/ 7 Macintosh	
Operating Environment	Depths down to – 60m	
Dimension	7 x 8,4 x 6 cm	
Weigh	170 g	

Table 2. Main characteristics of Intova camera

© GoPro HERO 2

Image Sensor	C-MOS	1 / 2.5"
Resolution	5M	2592 x 1944 pixel
Focal Length	5.0 mm	
Zoom	1X	
Opening Maximum	F/ 2.8 fixed focal – wide angle lens 170° - 8mm	
Supported System	Operating Macintosh - Mac OS X 10.4.11 Windows Vista / 7 / 8	
Operating Enviroment	– 80m	
Dimension	4,2 x 6 x 3 cm	
Weight	167g	

Table 3. Main characteristics of GoPro camera

4. IN SITU CAMERA CALIBRATION

The camera calibration has to be carried out in situ because of the extremely varying chemical and physical properties (salinity, temperature, density, etc.) of water, the medium the optical rays move across. In this analysis, it is assumed that within the very short period of the underwater phogrammetric survey these parameters, once determined, are invariant and can be used for the photogrammetric processing.

4.1 The frame for in situ camera calibration

The frame is used for two main purposes: to provide the known points for the orientation of the photograms and to execute the cameras calibration. The reference frame is composed of PVC bars which form approximately the edges of a parallelepiped of the following size: 0.9 x 0.2 x 0.15 m. The weight is about 3 kg (see Figure 4 and 5 for different perspective views of the calibration bar). The known points (targets) are signaled with a rectangular target, 30 mm wide, with alternate black and with cross printed. All targets materialized on the frame have been numbered and measured and the coordinates, x, y and z, determined (Table 4) in a reference system fixed on the frame. The measures have been performed by scanning the frame with a triangulation-based laser scanner © Konika Minolta RANGE 7 and identifying the center of each target on the three-dimensional model at very high accuracy (Figure 6). The positions of the targets were determined with an accuracy lower than 0.1 mm. The PVC thermal dilatation coefficient is about 7 ppm for °C. The variation of temperature from the surface to the working area at a depth of 15 m was about 5°C (13 °C versus 18 °C) that produces a potential (maximum) length variation of about 35 micron for the 1 m length of the bar. This variation is less than the GSD and precision that are expected from the photogrammetric acquisition.



Figure 4. Calibration frame (I)

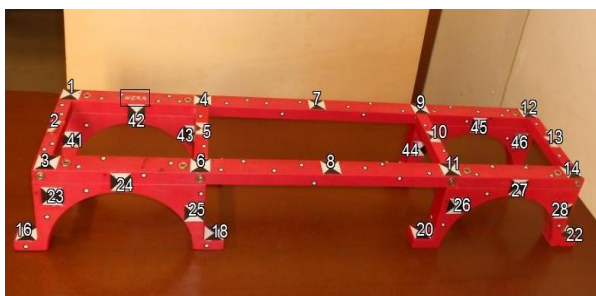


Figure 5. Calibration frame (II)



Figure 6. Calibration frame

Point	Position X metres	Position Y metres	Position Z metres
01	0.888134	0.0691786	0.1384361
02	0.893900	0.1520687	0.1385420
03	0.886535	0.2305210	0.1382356
04	0.678908	0.0691549	0.1371706
05	0.679326	0.1457817	0.1374712
06	0.678973	0.2304319	0.1371609
07	0.482592	0.0687632	0.1366616
08	0.485872	0.2298171	0.1372308
09	0.293082	0.0683195	0.1369745
10	0.293792	0.1470551	0.1373222
11	0.294089	0.2287728	0.1373911
12	0.079533	0.0670256	0.1378389
13	0.074352	0.1516373	0.1379888
14	0.079572	0.2280209	0.1380106
15	0.921320	0.0692769	0.0193975
16	0.922058	0.2336460	0.0209650
17	0.654221	0.0711048	0.0177473
18	0.653952	0.2326804	0.0182407
19	0.314423	0.0692246	0.0185597
20	0.313753	0.2306227	0.0178824
21	0.047200	0.0692796	0.0193975
22	0.046939	0.2282255	0.0193975
23	0.880074	0.2480730	0.9699460
24	0.788660	0.2467920	0.1209704
25	0.685318	0.2471323	0.0688813
26	0.275214	0.2463912	0.0840010
27	0.178558	0.2449525	0.1199609
28	0.080243	0.2453693	0.0752536
29	0.069372	0.0525437	0.0928352
30	0.183444	0.0518063	0.1186896
31	0.282701	0.0528066	0.0696801
32	0.693547	0.0541308	0.0917692
33	0.790057	0.0536941	0.1203303
34	0.888708	0.0537909	0.0760748
35	0.079651	0.2133120	0.0727988
36	0.182989	0.2134314	0.1207736
37	0.275613	0.2137860	0.0913263
38	0.686322	0.2154946	0.0714329
39	0.788505	0.2148392	0.1207429
40	0.879267	0.2160930	0.0921059
41	0.888642	0.0864214	0.0689297
42	0.783685	0.0857741	0.1204580
43	0.692949	0.0866900	0.0881470
44	0.282121	0.0850015	0.0686676
45	0.181107	0.0841090	0.1200876

Table 4. Target coordinates on the frame

4.2 3D Reconstruction on the frame model

Taking into account our choice to use the commercial software PhotoScan (©Agisoft), based on the Structure from Motion (SfM) approach (Ullman, 1979) and bundle adjustment, we have executed 12 photographs to portray the entire frame within each image. All acquisitions have been made at distance range of about 2 and 4 meters with a GSD (Ground Simple Distance) in the range about of 0.4 and 0.9 mm. Unfortunately, for the presence of a rocky block close to the frame (positioned near of the amphora, for subsequent photogrammetric survey), it was possible to photograph the frame mainly by a side only. The same procedure was performed for all three types of cameras. The SfM algorithm implemented by PhotoScan was used in this work to generate the dense point clouds of the frame. The reconstruction of objects by PhotoScan is a three-step process (Seitz, 2006). From a theoretical point of view, for a good reconstruction, at least two photographs representing a single point must be available. In this case, each point is represented in not less than 8 images. In the first step the alignment of the acquired images was performed. The SfM algorithm comes into play by the detection of image feature points (edges or others geometrical features) and reconstruction of their movement along the sequence of images. The SfM algorithm provides the basic geometry/structure of the scene, through the position of the numerous matched features, in addition to camera positions and internal calibration parameters. This is done in a local reference frame. In the second step a pixel-based dense stereo reconstruction was performed starting from the aligned dataset and sparse matching. After this step, fine topographic details available on the original images could be meshed (Mancini et al., 2013).

We collimated with accuracy (tens of micron at those image scale) all targets visible on all 12 frames available, repeating the

same operation with all 3 cameras. For each of the collimated targets the coordinates have been associated to the list of reference coordinates as previously determinate in the frame-fixed reference system and was assigned a constant weight (marker accuracy in photoscan) of 40 micron for each collimated marker. At the end, the bundle adjustment procedure, based on the least squares method, was launched and the calibration parameters determined by the model of Brown (Brown, 1971). The results could be retrieved by the final report provided and RMS (Root Means Square) on individual coordinates and the global RMS values inspected.

4.3 Determining camera calibration parameters

The calibration parameters determined for each of the three cameras are the following:

- fx, fy: focal length measured in pixels
- cx, cy: principal point coordinates
- sk: skew transformation coefficient
- k1, k2, k3, k4: radial distortion coefficients
- p1, p2: tangential distortion coefficients.

The calibration procedure provided the results hereafter summarized. Table 5 and 6 reports results about the calibration parameters and bundle adjustment errors for the ©Canon Power Shot G12 camera.

	Initial data (pix)	Adjusted (pix)
fx	3000.32	4103.91
fy	3000.32	4102.9
cx	1824	1848.48
cy	1368	1305.37
sk	0	10.8989
k1	0	0.103419
k2	0	0.321962
k3	0	0.482737
p1	0	-0.00107058
p2	0	-0.000228197

Table 5. Canon calibration parameters

Markers	Error (m)	Projections	Error (pix)
<input checked="" type="checkbox"/> 02	0.000949	10	0.565
<input checked="" type="checkbox"/> 03	0.000427	10	0.754
<input checked="" type="checkbox"/> 04	0.000279	10	0.534
<input checked="" type="checkbox"/> 05	0.000440	10	0.528
<input checked="" type="checkbox"/> 06	0.000639	10	0.671
<input checked="" type="checkbox"/> 07	0.000592	10	0.575
<input checked="" type="checkbox"/> 08	0.000425	10	0.505
<input checked="" type="checkbox"/> 09	0.000321	10	0.530
<input checked="" type="checkbox"/> 10	0.000121	10	0.714
<input checked="" type="checkbox"/> 11	0.000259	10	0.356
<input checked="" type="checkbox"/> 12	0.000665	10	0.624
<input checked="" type="checkbox"/> 13	0.000691	10	0.578
<input checked="" type="checkbox"/> 14	0.000270	10	0.444
<input checked="" type="checkbox"/> 16	0.000667	10	0.743
<input checked="" type="checkbox"/> 18	0.000797	9	0.497
<input checked="" type="checkbox"/> 20	0.000408	10	0.567
<input checked="" type="checkbox"/> 23	0.872855	10	0.438
<input checked="" type="checkbox"/> 24	0.000939	10	1.267
<input checked="" type="checkbox"/> 25	0.000065	10	0.707
<input checked="" type="checkbox"/> 26	0.000144	10	0.476
<input checked="" type="checkbox"/> 27	0.000448	10	0.433
<input checked="" type="checkbox"/> 28	0.000357	10	0.506
<input checked="" type="checkbox"/> 42	0.000372	9	0.577
<input checked="" type="checkbox"/> 45	0.000380	9	0.615
Total Error	0.000524		0.627

Table 6. Results of the bundle adjustment process for Canon camera

In Table 6 the flag means the point was included in the adjustment. As can be seen the maximum error is 0.939 mm whereas the average total error amount to 0.524 mm.

In Table 7 and 8 results from the calibration procedure and bundle adjustment errors are reported for the © Intova Sport HD.

	Initial data (pix)	Adjusted (pix)
fx	2778.13	4252.33
fy	5778.13	4252.33
cx	2000	1899.13
cy	1500	1524.97
sk	0	0
k1	0	-0.369359
k2	0	0.319438
k3	0	-0.0515793
p1	0	0
p2	0	0

Table 7. Intova calibration parameters

Markers	Error (m)	Projections	Error (pix)
01	0.00551	10	46.675
02	0.016166	10	46.672
03	0.021533	10	45.722
04	0.006307	10	46.599
05	0.009695	10	44.318
06	0.013537	10	43.188
07	0.005378	10	42.359
08	0.004622	10	40.027
09	0.009662	10	33.453
10	0.004810	10	32.973
11	0.008322	10	31.986
12	0.014069	10	21.154
13	0.001794	10	22.694
14	0.010930	10	24.427
16	0.021912	6	32.830
18	0.008798	10	31.970
20	0.013216	10	19.438
23	0.889805	10	41.982
24	0.016068	10	43.053
25	0.005842	10	36.637
26	0.007472	10	24.619
27	0.010075	10	24.618
28	0.003865	10	22.021
42	0.006465	10	45.154
45	0.012367	10	23.756
Total Error	0.011330		35.880

Table 8. Results of the bundle adjustment process for Intova camera

A maximum error of 9.551 mm can be detected from the table whereas the average total error is 11.330 mm. In Table 9 and 10 results from the calibration procedure and bundle adjustment errors are reported for the © GoPro HERO 2.

	Initial data (pix)	Adjusted (pix)
fx	3744.23	6573.37
fy	3744.23	6573.37
cx	1296	1285.84
cy	972	1042.99
sk	0	0
k1	0	-3.6244
k2	0	39.3978
k3	0	82.1368
p1	0	0
p2	0	0

Table 9. GoPro calibration parameters

Markers	Error (m)	Projections	Error (pix)
01	0.002594	12	3.999
02	0.002672	12	3.607
03	0.004611	12	3.811
04	0.038564	12	45.236
05	0.018481	12	24.283
06	0.021586	12	23.960
07	0.005531	12	3.503
08	0.001708	12	3.500
09	0.004787	12	3.137
10	0.002408	12	2.304
11	0.000901	12	2.351
12	0.002388	12	2.882
13	0.003696	12	2.584
14	0.004867	12	2.277
15	0.003077	12	3.116
16	1.230464	2	0.067
17	0.002740	12	2.152
18	0.002026	8	1.956
19	0.161218	10	1.540
20	0.163247	12	1.668
29	0.002717	12	2.640
30	0.003502	12	2.407
31	0.005102	12	1.862
32	0.003719	12	3.552
33	0.003491	12	3.870
34	0.002077	12	3.155
35	0.009558	8	1.395
36	0.001880	12	2.140
39	0.002688	12	3.435
40	0.007978	8	2.492
Total Error	0.043037		11.062

Table 10. Results of the bundle adjustment process for GoPro camera

A maximum error of 38.564 mm and an average total error of 43.037 mm into evidence.

Concerning the cameras Intova and GoPro, the tangential distortion parameters and skew turn out to be insignificant (Remondino and Fraser, 2006).

5. CONCLUSIONS

This paper aimed at comparing the performance of three cheap underwater cameras for metric applications. This evaluation was performed by analyzing the calibration parameters obtained under the same operating conditions. The shots were acquired at a sea depth of about 15 meters and a special calibration frame was used. By the application of a photogrammetric approach base on computer vision algorithms (SFM) and successive bundle adjustment, the calibration parameters of the three cameras were derived. These results are summarizing in Table 11 by using the total errors as a concise index.

	Error (mm)
Canon PowerShot G12	0.524
GoPro Hero2	43.037
Intova Sport HD	11.330

Table 11. Comparison of total errors related to used cameras

On the basis of what we obtained during this test, the so-called commercial action-cameras type GoPro and Intova exhibited unfavourable characteristics for underwater metric purpose. This is likely due to the strong distortion caused by lenses with very small focal length. The use of such kind of cameras for similar applications requires different models for the calculation of calibration parameters. To the contrary, the Canon camera, produced a total error which is compatible with most of the scopes of the underwater photogrammetry. Distortions detected for such camera are in many cases acceptable and well represented by the Brown's model and they are highlighted the behaviors to nonlinear optical projections of the cameras GoPro and Intova.

ACKNOWLEDGEMENTS

The authors thank Dr. Chiara Tagliatela (University of Bologna) for her contribution in the work of thesis and Dr. Isabella Toschi (FBK, Trento) for her valuable contribution.

REFERENCES

Brown D.C., 1971. *Close-Range Camera Calibration*. Photogr. Eng. 37: pp. 855-866

Capra A., 1992. *Non-conventional system in underwater photogrammetry*. I.S.P.R.S. Archives vol. XXIX, Comm.V, XVII I.S.P.R.S. International Congress, Washington, D.C. USA.

Capra A., 1994. *Application of underwater photogrammetry for the deformation control of submerged objects*. ISPRS Commission V (Melbourne), Vol.XXX, pp.16-22.

Caravalle A., Toffoletti I., 1997. *Anfore antiche. Conoscere e Identificarle*. pp. 98-99 Istituto ricerche ecologiche ed economiche Formello.

Drap P., Seinturie J., Long L., 2003. *Archaeological 3D modelling using digital photogrammetry and expert system. The case study of Etruscan amphorae*. The Sixth International Conference on Computer Graphics and Artificial Intelligence, May 2003, France.

Mancini F., Dubbini M., Gattelli M., Stecchi F., Fabbri S., Gabbianelli G., 2013. *Using Unmanned Aerial Vehicles (UAV) for High-Resolution Reconstruction of Topography: The Structure from Motion Approach on Coastal Environments*. Remote Sensing, 5 (12), 6880-6898.

Remondino F., Fraser C., 2006. *Digital camera calibration methods: consideration and comparisons*. International Archives of Photogrammetry, Remote Sensing and Spatial Information Sciences, Vol.36(B5), Dresden, Germany

Seitz S.; Curless B.; Diebel J.; Scharstein D.; Szeliski R. A 2006. *Comparison and Evaluation of Multi-View Stereo Reconstruction Algorithms*. In Proceedings of the 2006 IEEE Computer Society Conference on Computer Vision and Pattern, Washington, DC, USA. pp. 519–528.

Troisi S., Menna F., Nocerino E., Remondino F., 2013. *Il rilievo della falla della M/N Costa Concordia*. Proc. SIFET Conference, Catania, Italy

Ullman S., 1979. *The interpretation of structure from motion*. Proc. R. Soc. Lond. B 1979, 203, pp. 405–426.